

# Full Multigrid for Magnetostatics Using Unstructured and Non-Nested Meshes

Herbert De Gersem and Kay Hameyer

**Abstract**—Adaptive mesh refinement and mesh enhancing techniques, commonly applied in electromagnetic finite element simulation, give raise to a hierarchy of nonnested unstructured grids. The application of geometrical multigrid is not straightforward. The prolongation operator is adapted to the particular properties of the mesh refinement. Anti-symmetric boundary conditions and nonlinear material characteristics are incorporated. The numerical experiment performed on the model of a synchronous machine shows optimal convergence for the proposed multigrid scheme whereas the convergence of classical nested multigrid becomes troublesome.

**Index Terms**—Adaptive mesh refinement, finite element methods, iterative solvers, multigrid methods.

## I. INTRODUCTION

**F**INITE element simulation has found its way to the design and optimization of electrical apparatus. Unstructured finite element meshes allow an accurate description of the rather arbitrary geometries. A prescribed accuracy is achieved by adaptive mesh refinement based on error estimation, detecting, e.g., regions with ferromagnetic saturation.

Unstructured meshes and nonuniform mesh refinement are commonly used in electromagnetic simulation but cause a severe restriction to the application of conventional geometrical multigrid (MG) techniques, originally developed for uniformly refined, structured meshes. This paper deals with MG adjusted to arbitrarily refined meshes. In particular, the prolongation operator within the MG cycle is adapted to the nonnested hierarchy of meshes that naturally arise when mesh quality improvement techniques are applied.

The theory is developed using 2-D magnetostatic models. The partial differential equation  $-\nabla \cdot (\nu \nabla A_z) = J_z$ , with  $A_z$  and  $J_z$  the  $z$ -components of the magnetic vector potential and the current density respectively, and  $\nu$  the reluctivity, is discretized

applying first order linear triangular finite elements  $N_i(x, y)$ . The system matrix is  $\mathbf{K}\mathbf{x} = \mathbf{f}$  where

$$k_{ij} = \int_{\Omega} \nu \nabla N_i \cdot \nabla N_j d\Omega,$$

$$f_i = \int_{\Omega} J_z N_i d\Omega \quad \text{and} \quad x_j = A_{zj}.$$

## II. MULTIGRID

### A. Multigrid in Electromagnetic Simulation

MG methods became a standard solution method in many application areas [1]. MG approaches entered the field of quasi-static magnetic simulation a few years ago [2], [3]. Nowadays, research in the field is focused toward the development and application of algebraic MG schemes [4]–[6] and MG for 3-D *curl-curl* operator [7], [8]. Geometrical MG is fully mature to solve the Poisson equation arising from 2-D and 3-D nodal formulations for electro- and magnetostatics. Unfortunately, mainly uniformly refined meshes are considered [9]. Local, but nested, refinement is considered by a hierarchical MG method in [10]. Here, the MG idea is extended to nonnested hierarchies of locally refined meshes [11]. This research is motivated by the fact that nonuniform refinement, combined to mesh enhancing techniques, yielding nonnested grids, is particular advantageous and therefore commonly applied to electromagnetic simulation, featuring large relative differences in material properties and local nonlinear ferromagnetic phenomena.

### B. Multigrid Method

Linear iterative solvers are very effective to wipe out so called high frequent errors, i.e., errors occurring at small scales in the mesh [12]. Unfortunately, the long range errors decay only after a considerable number of iteration steps. The basic idea of MG consists of restricting the error to a coarser grid on which it appears again as a high frequent error and is therefore easily eliminated by an iterative solver on the coarser grid. A MG scheme is achieved if this concept is recursively applied to a hierarchy of grids, each of them wiping out the error components within the frequency bandwidth corresponding to its characteristic mesh size.

The procedure is depicted in Fig. 1. Solving  $\mathbf{K}\mathbf{x} = \mathbf{f}$  and starting from the iterand  $\mathbf{x}_h^k$  at iteration step  $k$  on a mesh with characteristic mesh size  $h$ , a few steps of a stationary iterative solver, such as, e.g., damped Jacobi or Gauss–Seidel, are applied as pre-smoothing, yielding  $\tilde{\mathbf{x}}_h$ . The coarse grid correction consists of restricting of the error  $\mathbf{e}_h = \mathbf{f} - \mathbf{K}\tilde{\mathbf{x}}_h$  to  $\mathbf{e}_H$  on

Manuscript received June 4, 2000.

This work was supported by the Belgian “Fonds voor Wetenschappelijk Onderzoek-Vlaanderen” (Project G.0427), the Belgian Ministry of Scientific Research (IUAP no. P4/20) and the research council of the K.U. Leuven.

H. De Gersem was with the Katholieke Universiteit Leuven, Department ESAT, Division ELEN and is now with the FB 18 Elektrotechnik und Informationstechnik, Fachgebiet Theorie Elektromagnetischer Felder, Darmstadt University of Technology, Schloßgartenstr. 8, D-64289 Darmstadt, Germany (e-mail: degersem@temf.tu-darmstadt.de).

K. Hameyer is with the Katholieke Universiteit Leuven, Department ESAT, Division ELEN, Kasteelpark Arenberg 10, B-3001 Leuven-Heverlee, Belgium (e-mail: kay.hameyer@esat.kuleuven.ac.be).

Publisher Item Identifier S 0018-9464(01)07845-1.

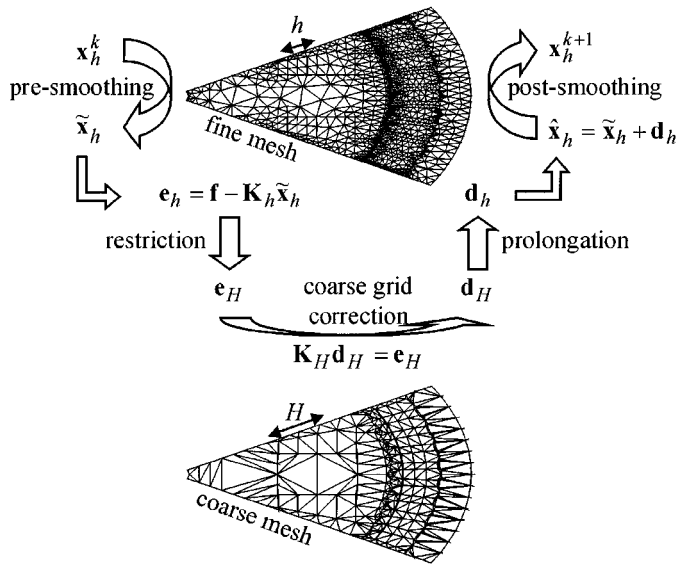


Fig. 1. One multigrid cycle.

a coarser grid with characteristic mesh size  $H$ , solving the defect equation  $\mathbf{K}_H \mathbf{d}_H = \mathbf{e}_H$ , with  $\mathbf{K}_H$  the system matrix defined on the coarser grid, and prolongating  $\mathbf{d}_H$  up to the defect  $\mathbf{d}_h$  on the finer grid. Finally, the defect is added to the iterand,  $\hat{\mathbf{x}}_h = \tilde{\mathbf{x}}_h + \mathbf{d}_h$  and a few post-smoothing steps are applied, yielding the new iterand  $\mathbf{x}_h^{k+1}$ .

The particular MG cycle, used here, consists of one Gauss–Seidel pre-smoothing step, the restriction defined by the adjoint of the prolongation, the coarse grid correction, the prolongation and 1 Gauss–Seidel post-smoothing step. If the concept is applied recursively, a hierarchy of finite element (FE) meshes is required. A V- or W-cycle correspond to one or two MG cycles respectively, performed on each level [12]. Here, V-cycles are used. On the coarsest level, the system is solved exactly by an LU-decomposition. A full MG method is achieved if the coarser levels serve also to determine an initial estimate for the MG solver at the finer discretizations [12].

### C. Non-Linear Multigrid

If ferromagnetic saturation is considered, a Newton–Raphson linearization is invoked. Due to the changes in the system to be solved at each Newton step, a slightly different approach is required. The most recently obtained nonlinear information, that is gathered in the Jacobian, is transferred to the coarser grids by the Galerkin approach. The Jacobian on a coarser grid is

$$\mathbf{J}_H = \mathbf{P}_h^* \mathbf{J}_h \mathbf{P}_h, \quad (1)$$

with  $\mathbf{J}_h$  the Jacobian on the grid and  $\mathbf{P}_h$  the coarse-to-fine grid prolongation operator. The MG cycle remains essentially unchanged. The increased computational work during set-up is negligible with respect to the cycling time itself.

### D. Convergence of Multigrid

The convergence properties of MG depend on the proper blend of smoothing and coarse grid correction. For each bandwidth of error components, an appropriate grid on which

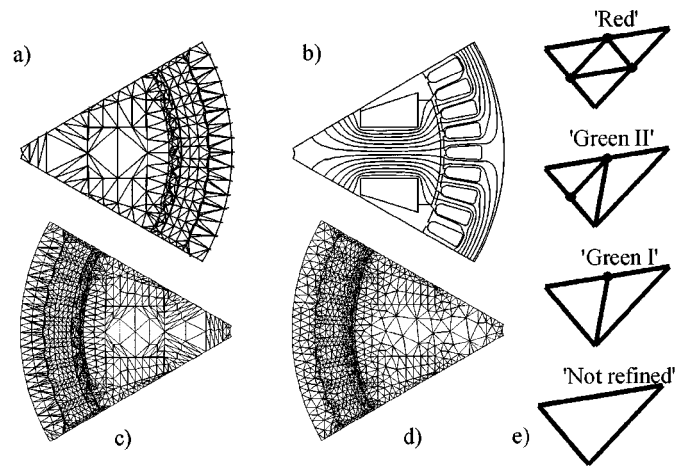


Fig. 2. (a) Coarsest mesh, (b) magnetic flux lines of an intermediate solution, (c) nested refined mesh and (d) mesh refined with aspect ratio enhancement of a one-pole synchronous machine model; (e) nonuniform mesh refinement.

the components vanish by a few smoothing steps, has to be provided. Convergence proofs and estimates rely upon the inclusion of the coarser finite element spaces within the finer ones. In that case, weak forms of the partial differential equation can be inherited from one space to the other and optimal convergence is proved [13]. In the case of nonnested grid, the spaces are also nonnested and the convergence proof has to rely upon regularity conditions to which the applied MG cycle has to be tuned [13].

## III. NON-UNIFORM MESH REFINEMENT

Relevant electromagnetic models usually require unstructured meshes to resolve for all geometrical details [Fig. 2(a)]. To achieve a prescribed accuracy, adaptive mesh refinement is applied. An *a-posteriori* error estimator applied to an intermediate solution [Fig. 2(b)], indicates the elements with large magnetic fields, large energies, large gradients or high levels of saturation. Only the fraction of elements with the highest errors, is marked for refinement. Edges in between marked elements are refined, causing nonuniform refinement [Fig. 2(e)]. Non-uniform mesh refinement, however, tends to worsen the shapes of the finite elements [Fig. 2(c)]. Large angles are to be avoided from the numerical point of view [14], [15]. Therefore, quality enhancement for the mesh is appropriate. Since adaptive mesh refinement is inevitably nonuniform and because of the use of unstructured grids itself, the prolongation operator is much more complicated when compared to the one between structured and uniformly refined meshes. Moreover, because of additional mesh enhancement, two successive meshes are not longer nested [Fig. 2(d)]. The MG scheme has to deal with restriction and prolongation operators between nonnested meshes.

### A. Edge Swapping

To avoid large angles within the mesh, the Delaunay property is approximately imposed. The Cline and Renka test is applied to all edges whether swapping them would decrease the aspect ratio [16] [Fig. 3(a)]. A Delaunay triangular would be achieved

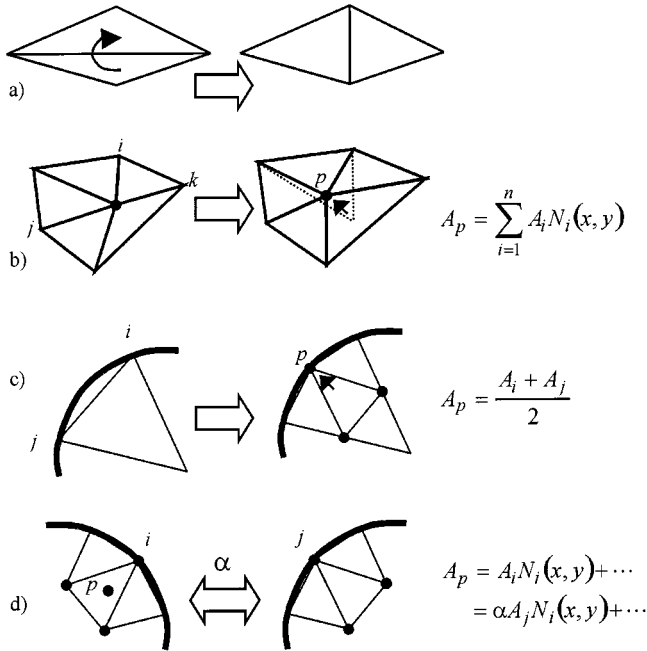


Fig. 3. Adjustments of the prolongation operator according to (a) swapping edges; (b) moving nodes; (c) restoring the original geometry; (d) periodic boundary conditions.

if this procedure is repeated until all edges fulfill the test. Proceeding until the number of swapped edges is only a fraction of the number of edges, already yields a considerable improvement of the mesh quality [16]. Because of the nodal formulation applied here, swapping edges does not affect the restriction and prolongation operators.

### B. Moving Nodes

To attain a smooth transition from areas with tiny elements to roughly discretized ones, interior nodes of the mesh are moved to the centers of the control volumes formed by their surrounding elements [Fig. 3(b)]. This is done by passing through the list of nodes until less than a certain percentages of nodes have to be moved. The prolongation is affected by this procedure. The common prolongation defined by linear interpolation between two nodes,

$$A_p = \frac{A_j + A_k}{2}, \quad (2)$$

is not longer valid. Instead, a defect computed on a coarser grid is prolonged to a finer grid by a projection applying the shape functions to obtain the value at interior nodes [17]:

$$A_p = \sum_{i=1}^n A_i N_i(x_p, y_p). \quad (3)$$

To avoid searching in the mesh during the MG cycles, the prolongation operator is constructed during the set-up phase. To reduce the cost of the prolongation operator, only dependencies beyond a certain threshold, e.g.,  $N_i(x_p, y_p) > 0.01$ , are admitted to the prolongation stencils.

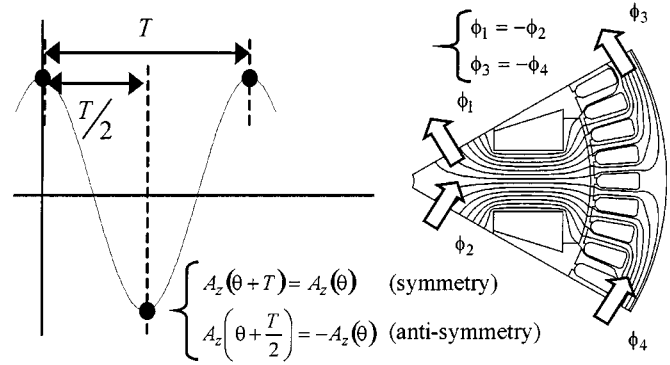


Fig. 4. Periodic boundary conditions applied to a one-pole model of a 6-pole synchronous machine with periodicity  $T$  along the air gap measured by  $\theta$ .

### C. Restoring the Original Geometry

While refining the mesh, nodes are redirected in order to restore the original geometry at curved boundaries [Fig. 3(c)]. For the construction of the prolongation operator, two situations are distinguished. If the material properties of the domains at both sides of the boundary are about the same, the aforementioned weighting for moved nodes is imposed:

$$A_p = \sum_{i=1}^n A_i N_i(x_p, y_p). \quad (4)$$

If however, the curved boundary separates regions with a large relative difference in permeability, e.g., iron and air, the weighting formula would prolongate as if the new node is created within one of both regions instead of upon the boundary. Here, linear interpolation is more appropriate:

$$A_p = \frac{A_i + A_j}{2}. \quad (5)$$

## IV. PERIODIC BOUNDARY CONDITIONS

The geometries and the excitations of electrical devices are often periodic in space. Hence, the computational domain can be reduced to, e.g., half or one quarter of the device (Fig. 4). A periodic boundary condition relates the potential values on two boundaries  $\Gamma_1$  and  $\Gamma_2$  to each other:

$$A|_{\Gamma_1} + \alpha A|_{\Gamma_2} = \beta. \quad (6)$$

The most common periodic boundary conditions are symmetry ( $\alpha = -1; \beta = 0$ ) and anti-symmetry ( $\alpha = 1; \beta = 0$ ). To retain the symmetry of the system matrix, the degrees of freedom at the *slave* boundary are eliminated with respect to those at the *master* boundary according to (6). The prolongator has to incorporate the connectivity of the periodic boundary conditions in the prolongation stencils for newly created nodes neighboring the slave boundary nodes [Fig. 3(d)]. If periodic boundaries are applied to model an open boundary transformation, e.g., the Kelvin transformation, a more elaborated approach is required [18].

## V. APPLICATION

The MG solver is applied to a model of a synchronous generator with six salient poles (Fig. 2). The gradient of the magnetic

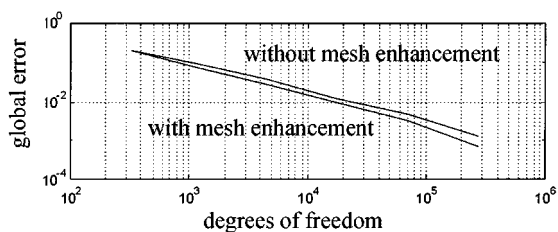


Fig. 5. Global error convergence of nested and nonnested mesh adaptation.

TABLE I

ITERATION COUNTS FOR NESTED AND NON-NESTED MG COMPARED TO SYMMETRIC SUCCESSIVE OVERRELAXATION (SSOR) AND INCOMPLETE CHOLESKY (IC) PRECONDITIONED CONJUGATE GRADIENTS (CG)

Step	#nodes	Non-nested MG	Nested MG	SSORCG	ICCG
0	331	-	-	92	67
1	1160	19	44	176	113
2	4501	19	48	333	216
3	17729	19	78	653	434
4	70369	18	86	1286	872
5	280385	17	92	2540	1763

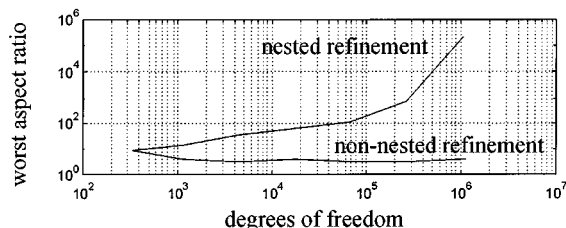


Fig. 6. Worst aspect ratio of nested and nonnested nonuniform refinement.

flux density, serves as an error estimator. The total magnetic energy stored in the devices is applied as global error criterion. Enhancing the mesh during adaptation improves the convergence of the global error (Fig. 5). For this particular model, 0.5% accuracy is attained with  $10^5$  degrees of freedom applying nonnested grids instead of  $2 \cdot 10^5$  for the nested ones. This fact motivates the use of mesh enhancement in electromagnetic simulation.

The MG, applied to nonuniformly refined, nonnested meshes as proposed here, requires much less cycles to converge when compared to nested MG (Table I). Non-uniform refinement without mesh enhancement, creates a nested hierarchy of grids. The worst aspect ratio's of the elements, however, increase (Fig. 6). They are responsible for a considerable increase of the spectral radius of the iteration matrices corresponding to the Gauss-Seidel smoothers at the fine meshes. Hence, the smoothing properties deteriorate and the optimal convergence of MG is lost. The quality improvement of the mesh, thanks to moving nodes and swapping edges, retains acceptable angles in the mesh and thus the good smoothing properties and a constant number of MG cycles at each level of adaptation.

In the case of nonnested MG, the prolongation operator is much more expensive. This does, however, not harm the performance of nonnested MG. Timings are compared in Fig. 7 and clearly indicate the benefits of nonnested MG over nested MG and the preconditioned Conjugate Gradient iterative method. As an indication, the slope corresponding to optimal complexity is added to Fig. 7.

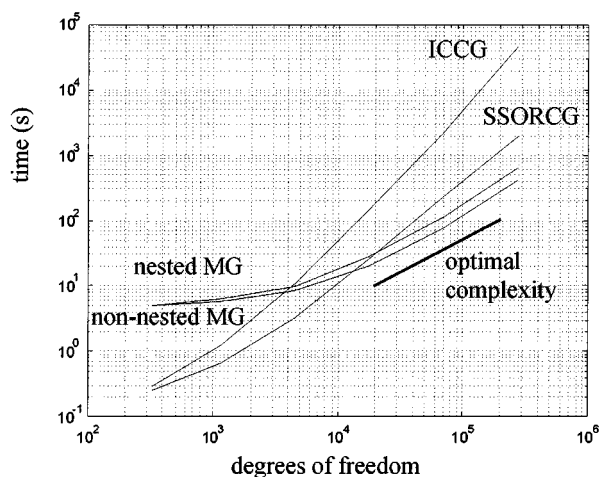


Fig. 7. Cumulative timings of nested and nonnested MG compared to SSORCG and ICCG.

## VI. CONCLUSIONS

The application of multigrid to a nonnested hierarchy of unstructured meshes requires particular adjustments of the prolongation operator according to moved nodes, restoration of the original geometry at curved boundaries and periodic boundary conditions. The decrease of the aspect ratio's of the finite elements peculiar to nonuniform refinement, causes a deteriorating convergence of MG. The nonnested full MG scheme overcomes this by mesh enhancement and combines a better convergence of the global error to faster iterative solutions of the linear systems when compared to nested MG.

## REFERENCES

- [1] C. C. Douglas, "Multigrid methods in science and engineering," *IEEE Computational Science in Engineering*, vol. 3, pp. 55–68, 1997.
- [2] I. Tsukerman, "Fast finite element solvers for problems with magnetic materials," *IEEE Trans. Magn.*, vol. 29, no. 6, pp. 2365–2367, Nov. 1993.
- [3] C.-S. Koh, K. Choi, and S.-Y. Hahn, "An adaptive finite element scheme using multi-grid method for magnetostatic problems," *IEEE Trans. Magn.*, vol. 25, no. 4, pp. 2959–2961, July 1989.
- [4] R. Mertens, H. De Gersem, R. Belmans, K. Hameyer, D. Lahaye, S. Vandewalle, and D. Roose, "An algebraic multigrid method for solving very large electromagnetic systems," *IEEE Trans. Magn.*, vol. 34, no. 5, pp. 3327–3330, 1998.
- [5] D. Lahaye, H. De Gersem, S. Vandewalle, and K. Hameyer, "Algebraic multigrid for complex symmetric systems," *IEEE Trans. Magn.*, submitted for publication.
- [6] M. Kaltenbacher, S. Reitzinger, and J. Schöberl, "Algebraic multigrid for solving 3D nonlinear electrostatic and magnetostatic field problems," *IEEE Trans. Magn.*, submitted for publication.
- [7] R. Hiptmair, "Multigrid method for  $H(\text{DIV})$  in three dimensions," *Electronic Trans. Numer. Analysis*, vol. 6, pp. 133–152, Dec. 1997.
- [8] M. Schinnerl, J. Schöberl, and M. Kaltenbacher, "Nested multigrid methods for the fast numerical computation of 3D magnetic fields," *IEEE Trans. Magn.*, submitted for publication.
- [9] V. Cingoski, K. Tsubota, and H. Yamashita, "Investigation of the efficiency of the multigrid method for finite element electromagnetic field computations using nested meshes," *IEEE Trans. Magn.*, vol. 35, no. 5, pp. 3751–3753, Sept. 1999.
- [10] I. Tsukerman and A. Plaks, "Hierarchical basis multilevel preconditioners for 3D magnetostatic problems," *IEEE Trans. Magn.*, vol. 35, no. 3, pp. 1143–1146, May 1999.
- [11] V. Cingoski, K. Tsubota, and H. Yamashita, "Comparison between nested and nonnested multigrid methods for magnetostatic field analysis," in *ISEM'99*, Pavia, Italy, May 10–12, 1999.

- [12] W. Hackbusch, *Multi-Grid Methods and Applications*. Berlin: Springer-Verlag, 1985.
- [13] J. H. Bramble, *Multigrid Methods*. Harlow: Longman, 1993.
- [14] I. Babuška and A. K. Aziz, "On the angle condition in the finite element method," *SIAM J. Numer. Analysis*, vol. 13, no. 2, pp. 214–226, April 1976.
- [15] I. Tsukerman, "A general accuracy criterion for finite element approximation," *IEEE Trans. Magn.*, vol. 34, no. 5, pp. 2425–2428, September 1998.
- [16] R. Mertens, U. Pahner, R. Belmans, and K. Hameyer, "Selected projection methods to improve the convergence of nonlinear problems," *COMPEL*, vol. 18, no. 4, pp. 638–646, 1999.
- [17] R. Mertens, U. Pahner, H. De Gersem, R. Belmans, and K. Hameyer, "Improving the overall solver speed: A fast, reliable and simple adaptive mesh refinement scheme," in *4th Int. Workshop on Electric and Magnetic Fields*, Marseille, France, May 12–15, 1998, pp. 385–390.
- [18] A. Plaks, I. Tsukerman, S. Painchaud, and L. Tabarovsky, "Multigrid methods for open boundary problems in geophysics," *IEEE Trans. Magn.*, July 2000, submitted for publication.